

Confined Impinging Jets in Porous Media

B Buonomo, L Cirillo, O Manca, N Mansi, S Nardini¹

Dipartimento di Ingegneria Industriale e dell'Informazione,
Seconda Università degli Studi di Napoli (SUN),
Via Roma 29, Aversa (CE), 81031, Italia

email: sergio.nardini@unina2.it

Abstract. Impinging jets are adopted in drying of textiles, paper, cooling of gas turbine components, freezing of tissue in cryosurgery and manufacturing, electronic cooling.

In this paper an experimental investigation is carried out on impinging jets in porous media with the wall heated from below with a uniform heat flux. The fluid is air. The experimental apparatus is made up of a fun systems, a test section, a tube, to reduce the section in a circular section. The tube is long 1.0 m and diameter of 0.012 m. The test section has a diameter of 0.10 m and it has the thickness of 10, 20 and 40 mm. In the test section the lower plate is in aluminum and is heated by an electrical resistance whereas the upper plate is in Plexiglas. The experiments are carried out employing a aluminum foam 40 PPI at three thickness as the test section. Results are obtained in a Reynolds number range from 5100 to 15300 and wall heat flux range from 510 W/m² to 1400 W/m². Results are given in terms of wall temperature profiles, local and average Nusselt numbers, pressure drops, friction factor and Richardson number.

Nomenclature

D	diameter (mm)
EPR	efficiency
f	friction factor
Gr	Grashof number
H	slot height (mm)
k	thermal conductivity (W m ⁻¹ K ⁻¹)
Nu	Nusselt number
P	Pressure
\dot{q}	heat flux (W m ⁻²)
PPI	pores per inch
Re	Reynolds number
Ri	Richardson number
T	temperature (°C)
V	air velocity (m s ⁻¹)

Greek symbols

ρ	density (kg m ⁻³)
ε	porosity
μ	kinematic viscosity (kg m ⁻¹ s ⁻¹)
ν	dynamic viscosity

Subscripts

s	clean
c	convective



1. Introduction

Aluminium foams with high thermal conductivity is an effective method of heat transfer enhancement due to their low weight, good strength, rigidity, damping of vibrations and noise, shock resistance [1]. In several applications in the literature, the metal foams were used in heat exchangers because of its high transfer capabilities. Boomsma et al. [2] carried out an experimental analysis on compact heat exchanger with open-cell metal foam. Their results show that metal foam heat exchangers have thermal resistances that are almost one-third of the available conventional heat exchanger. Metal foam have a high ratio between surface area and pressure drop, and with uniform lower density. The pressure drop is lower than in ceramic structures when considering the unit of volume [3]. Leong and Jin [4, 5] carried out an experimental investigation on an oscillating flow through a rectangular channel filled with open-cell metal foam. They analyzed rectangular channel with 10, 20 and 40 PPI (pores per inch) aluminium foam and they gave results on pressure drops and air velocities. They show that the oscillating flow features in an open-cell metal foam were governed by the kinetic Reynolds number Re based on a hydraulic diameter and the dimensionless flow displacement amplitude ADh . Subsequently, they used the porous media to obtain the heat transfer performance of metal foam heat sinks subjected to oscillating flows of various frequencies. Their results shown that for length-averaged Nusselt number for both oscillating and steady flows, higher heat transfer rates could be obtained when metal foams have subjected to oscillating flow. A one dimensional numerical analysis of heat transfer of metal foams has carried out by Dukhan et al. [6] that have considered only one pore density, 10 PPI. This analysis showed that the temperature decreases exponentially along the foam in the flow direction. Feng et al. [7] have carried out an experimental and numerical investigations on finned metal foam and metal foam. They have analysed an aluminium foam of 96.3% porosity and 8 PPI with four 2 mm-thickness plate fins. Their results were shown in terms of heat transfer and pressure drop. Experimental results show that under a given flow rate condition, as the foam height increases, the heat transfer of metal foam heat sinks decreases monotonously whilst that of finned metal foam heat sinks first increases and then slightly decreases. Jeng and Tzeng have investigated numerically impinging cooling of metal foams under a confined slot jet. Subsequently, the same authors have carried out an another study considering foam tip bypass flow, both experimentally and numerically [8-10]. Kim et al. [11] have analysed experimentally heat transfer of aluminium foams under multi-air jet impingement, while, Kuang et al. [12] have investigated the effects of foam height and jet to foam distance on heat transfer of metal foams under an axial fan flow. Marafie et al. [13] have carried out a numerical analysis of the non-Darcian effects on the mixed convection heat transfer in a metal foam block with a confined slot jet. Their results show that the Nusselt number increases with decreasing dimensionless height of the foam block up to 0.05, below which the Nusselt number decreases. Shih et al. [14] have investigated experimentally the heat transfer characteristics of aluminium foam heat sinks with restricted flow outlets under impinging jet flow conditions. They have noted that the increase of the Nusselt number of the aluminium foam heat sink with the decrease in the flow outlet height is caused by the reduced convective resistance at the solid-gas interface through the increased velocity near the heat generation surface. Di Bella et al. [15] have realized a flow visualization study of the jet dynamics in a round jet impinging on a foamed aluminium porous media. They have found that the penetration of the impinging flow into the porous media is significantly affected by permeability. As permeability decreases, flow deflection off the impact surface of the foam increases, approaching the fluid dynamics behaviour of impact on a solid cube. Rallabandi et al. [16] have studied the heat transfer enhancement in rectangular channels with axial ribs or porous foam under through flow and impinging jet conditions. They have noted that the porous media shows a more significant increase in heat transfer coefficient for both channel flow and impingement cases. Imraan and Sharma [17] have carried out a CFD analysis of jet impingement heat transfer in a frost free refrigerator. They have investigated for Reynolds number in the range of 1 000 and 12 000. Their results show that the slot jet impinging on a circular cylinder in a

confined space yields heat transfer rates that are between those for the corresponding uniform cross-flow and slot jet impingement on a non-confined cylinder. Huang and El Genk [18] have carried out an experimental analysis on heat transfer of an impinging jet on a flat surface to determine the values of the local and average Nusselt numbers, in particular for low values of Reynolds number and jet spacing. The main aim of this experimental analysis is to analyse the flow and the heat transfer features of an impinging jet with aluminium foam of 40 PPI, wall heated from below with a uniform heat flux. The aim is to obtain values of friction factor and heat transfer for three different configurations. The metal foam analysed are 10, 20 and 40 mm thick. It was investigated with Reynolds number ranging from 5100 to 15300 and a uniform wall heat flux equal to 510 W/m^2 , 765 W/m^2 , 1020 W/m^2 and 1400 W/m^2 . The results show wall temperature profiles, air temperature, local and average Nusselt numbers, pressure drop, friction factor.

2. Apparatus

The experimental apparatus includes the test section, instruments and air facility. A fan sends the air from the laboratory room to the jet through a flow rate measurement system. The flow rate is measured with rotameter Krohne type VA40S and it is regulated by a valve (Fig.1a).

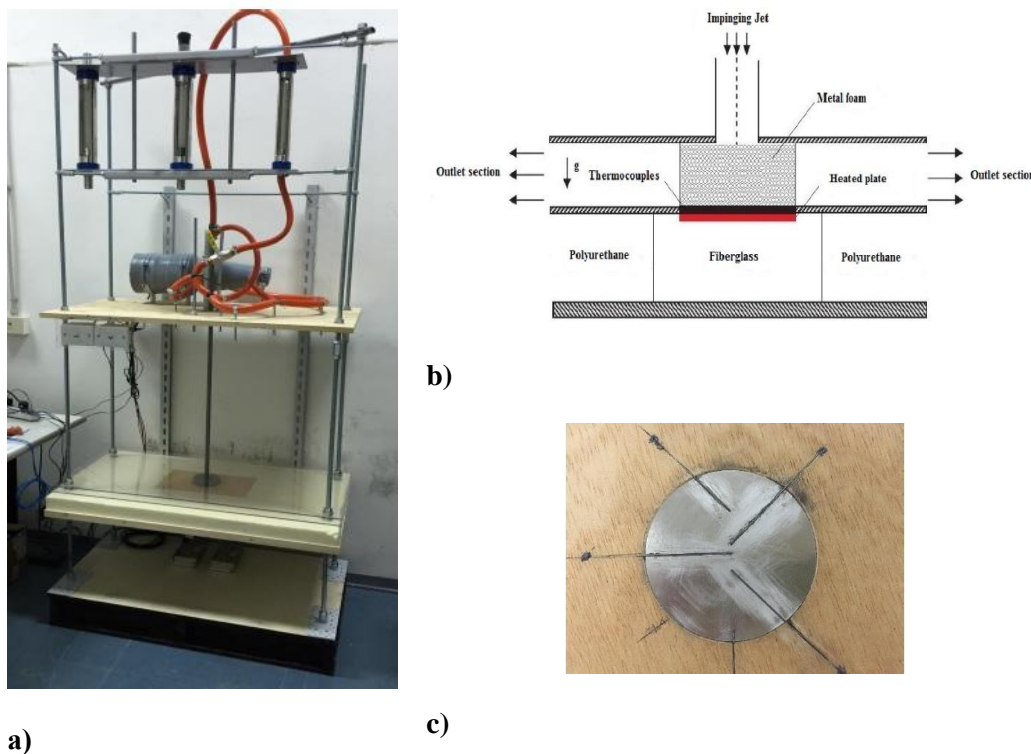


Figure 1. Experimental apparatus: a) fan system; b) sketch of impinging jet of metal foam; c) thermocouples position

The flow enters in the outlet duct with a diameter of 12 mm and 1 m long. In the second part the jet impinges the metal foam superiorly and inferiorly confined by two Plexiglas plates 4 mm thick. The metal foam has been positioned on an aluminium plate (3 mm thick). The aluminium foam heated from below by means of an electrical resistance RS Components IT 245-590 18 Ohm regulated by a power supply AGILENT E3633A. To reduce heat losses, a polystyrene block and fiberglass is affixed to bottom face of heated plate (Fig. 1c). Temperatures were measured by thermocouples (type J). An Isotech instrument mod. 938 ice point, with an accuracy of $\pm 0.04 \text{ }^{\circ}\text{C}$ and 50 channels, was used as thermocouple reference junctions. The thermocouples had been calibrated before their installation. 5 thermocouples were deployed along the diameter of the aluminum plate and 2 in the outlet section of impinging jet to measure the air temperature of jet (Fig.2). An AGILENT 34980A multifunction measurement unit and a computer were used for the

data acquisition. The porous media that filled the test section is aluminum foam of three different geometric specifications: 40 PPI with thickness of 10, 20 and 40 mm. The range of the Reynolds number varied from 5100 to 15300. To acquire the data of pressure a digital manometer tube has been used.

3. Data redaction

In this paper, the tests have been performed by variation of the Reynolds number 5100 – 15300. The average and local Nusselt number were determined as functions of parametric values of the Reynolds,

$$Nu_i = \frac{q_c D}{(T_{wi} - T_o) k_{air}} \quad (4)$$

the subscript i indicates the axial location on the wall (index w) at which the temperature is being measured. T_o is a reference temperature. It is the temperature of the air at the inlet of the heated test section which is a known quantity. It is convenient to use it in the evaluation of the Nusselt number in order to obtain the heat transfer coefficient. D is the diameter of the impinging jet, q_c is the wall heat flux and k_{air} is the thermal conductivity of the air. The average Nusselt number was calculated by:

$$Nu = \frac{q_c}{T_w - T_o} \frac{D}{k_{air}} \quad (5)$$

The Nusselt number results will be plotted as a function of Reynolds number, defined:

$$Re = \rho V D \mu^{-1} \quad (6)$$

Where H is the height of the slot (10, 20 and 40 mm) and Therefore, it has been evaluated the pressure drop ΔP at upstream and downstream of the test section and then it has been evaluated the friction factor with the equation:

$$f = \Delta P (\rho V^2 0.5)^{-1} \quad (7)$$

To evaluate the improvement due to the presence of the metal foam, it is necessary a quantitative methodology. In this work, EPR has been evaluated comparing the performances of surface with and without foams:

$$EPR = \overline{Nu} Nu_s^{-1} (ff_s^{-1})^{-0.33} \quad (8)$$

With Nu_s and f_s is average Nusselt number and friction factor of the smooth surface respectively.

3.1 Uncertainty

Analysis of the uncertainties on the measured parameters are $\pm 0.3^\circ\text{C}$ for temperature and $\pm 1\%$ for pressure. The uncertainty of Nusselt number, Reynolds number, friction factor and EPR have been evaluated with the Kline and McClintock [19] methodology. It has been estimated that the uncertainty of the Nusselt number is $\pm 2.5\%$, the Reynolds number is $\pm 4.3\%$, EPR is $\pm 4.8\%$ and friction factor is $\pm 3.1\%$.

4. Results

This experimental investigation has been carried out with air. The results have been presented as a function of Reynolds number and thermocouples position. The temperature profile at three

different configurations and a comparison of temperature profile between case clean and case with heat flux at 1020 W/m^2 , is plotted in fig. 2 (a-d).

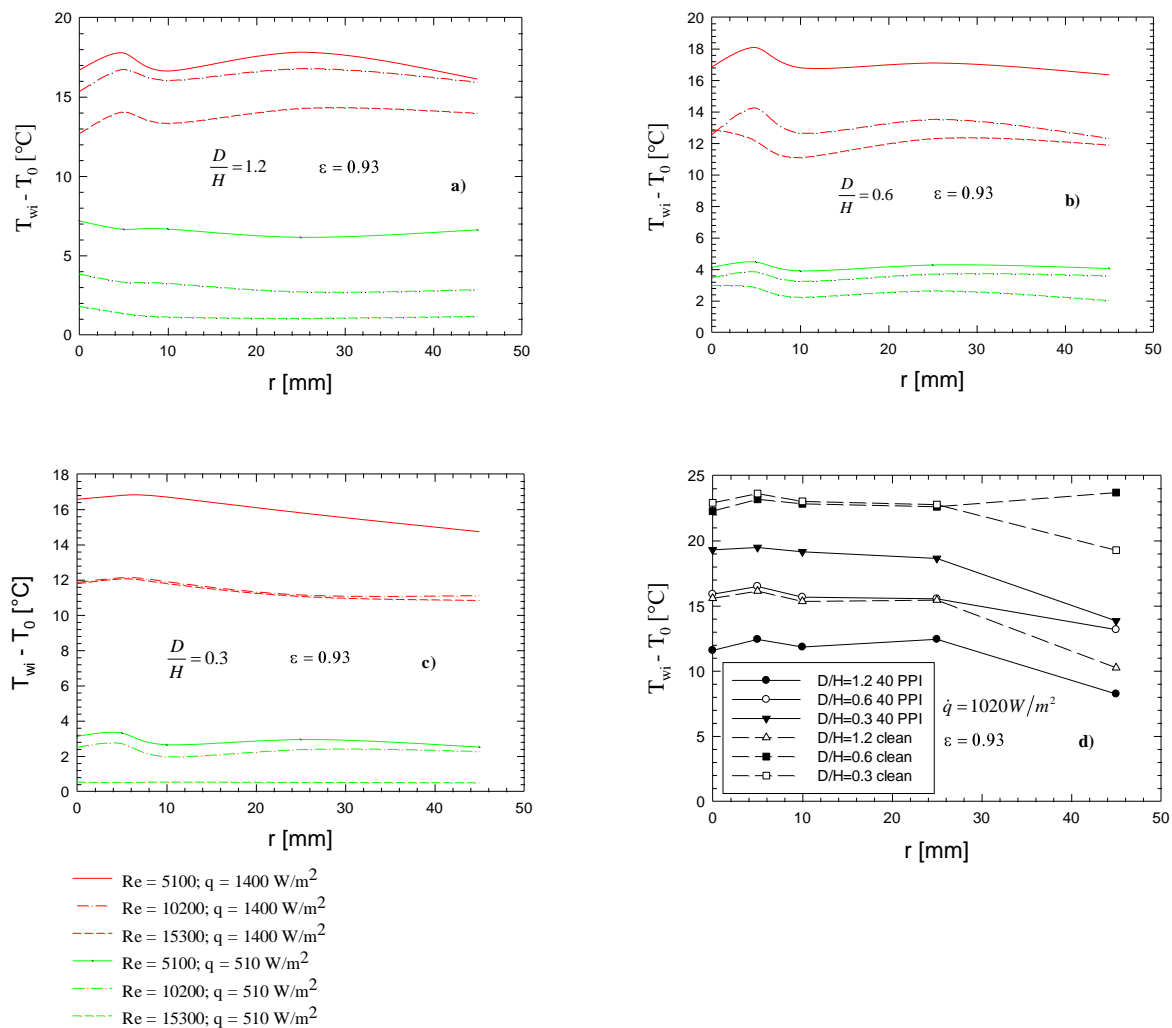


Figure 2. Temperature profile: a) $D/H = 1.2$; b) $D/H = 0.6$; c) $D/H = 0.3$; d) comparison between case clean and with metal foam.

These graphs show that the ratio D/H is important. In fact, at low D/H values, the metal foam determines a minimal wall temperature at Reynolds number equal to 10200 and 15300. Besides, the metal foam has generated a ΔT equal to 5-7 °C between case clean and with porous media. Fig. 3 (a-d) compares local Nusselt number as a function of abscissa r for different configurations. Fig. 3 shows that the convective heat transfer increases with the mass flow rate, in fact, the local Nusselt number is higher for higher values of Reynolds number. Therefore, for $\dot{q} = 510 \text{ W/m}^2$ and for $r = 45 \text{ mm}$ the convective phenomena are predominant on those conductive.

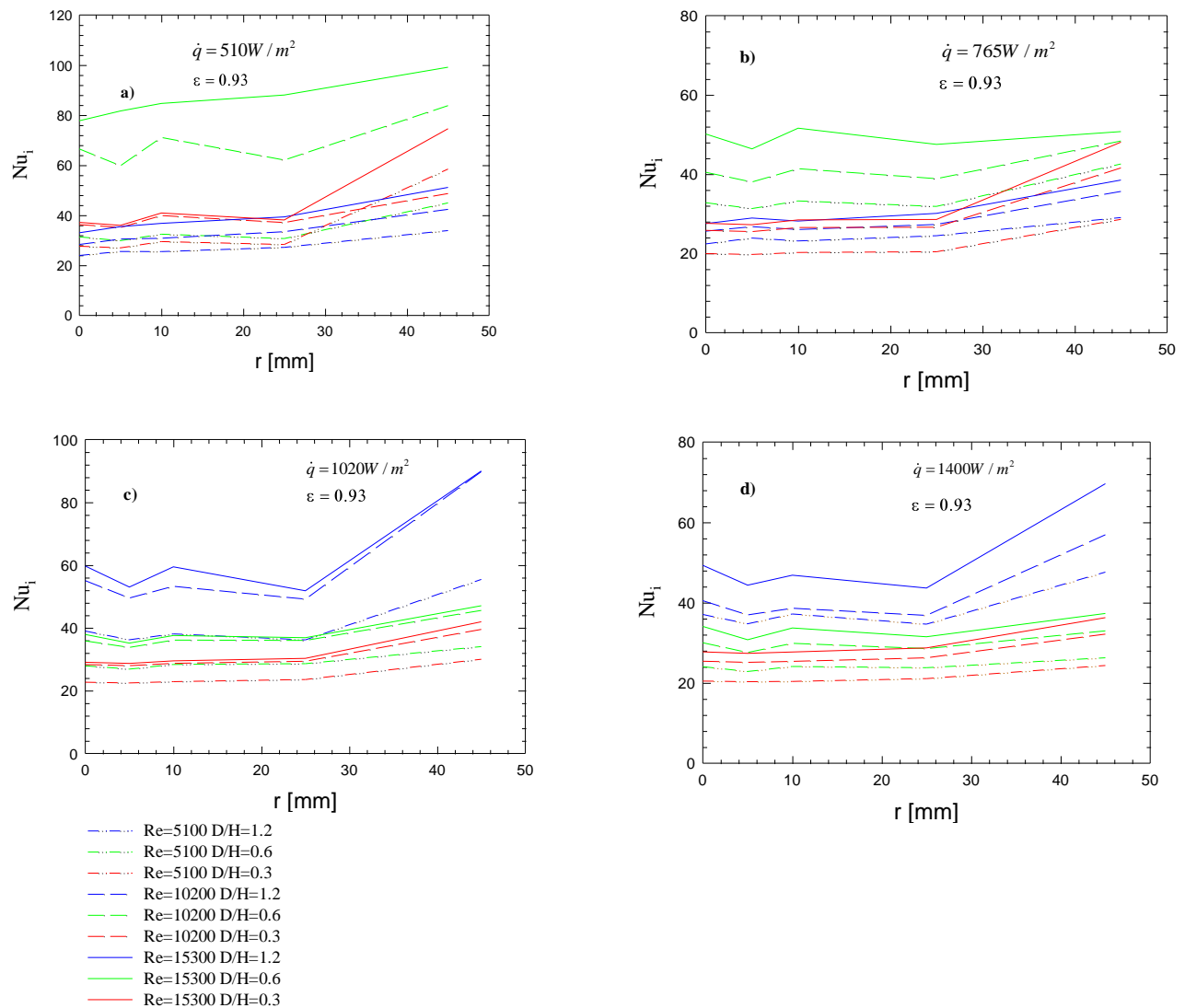


Figure 3. Local Nusselt number: a) $\dot{q} = 510 \text{ W/m}^2$; b) $\dot{q} = 765 \text{ W/m}^2$; c) $\dot{q} = 1020 \text{ W/m}^2$; d) $\dot{q} = 1400 \text{ W/m}^2$

Fig. 4 (a, d) shows clearly that increasing the Reynolds number the average Nusselt number increases. For low wall heat flux values the average Nusselt number is higher for D/H values equal to 0.6 and for high wall heat flux values the average Nusselt number is higher for D/H values equal to 1.2. Figure 5 (a-b) shows pressure drop and the friction factor as a function of Reynolds number. It is evident an increase of pressure drop increasing velocity of the flux. Higher value is 101 Pa and 15300 Re. The friction factor is a function of pressure drop, but the air velocity grows faster and then the trend of friction factor decrease with Reynolds number. The values higher of friction factor occur for Reynolds number equal to 5100 with metal foam.

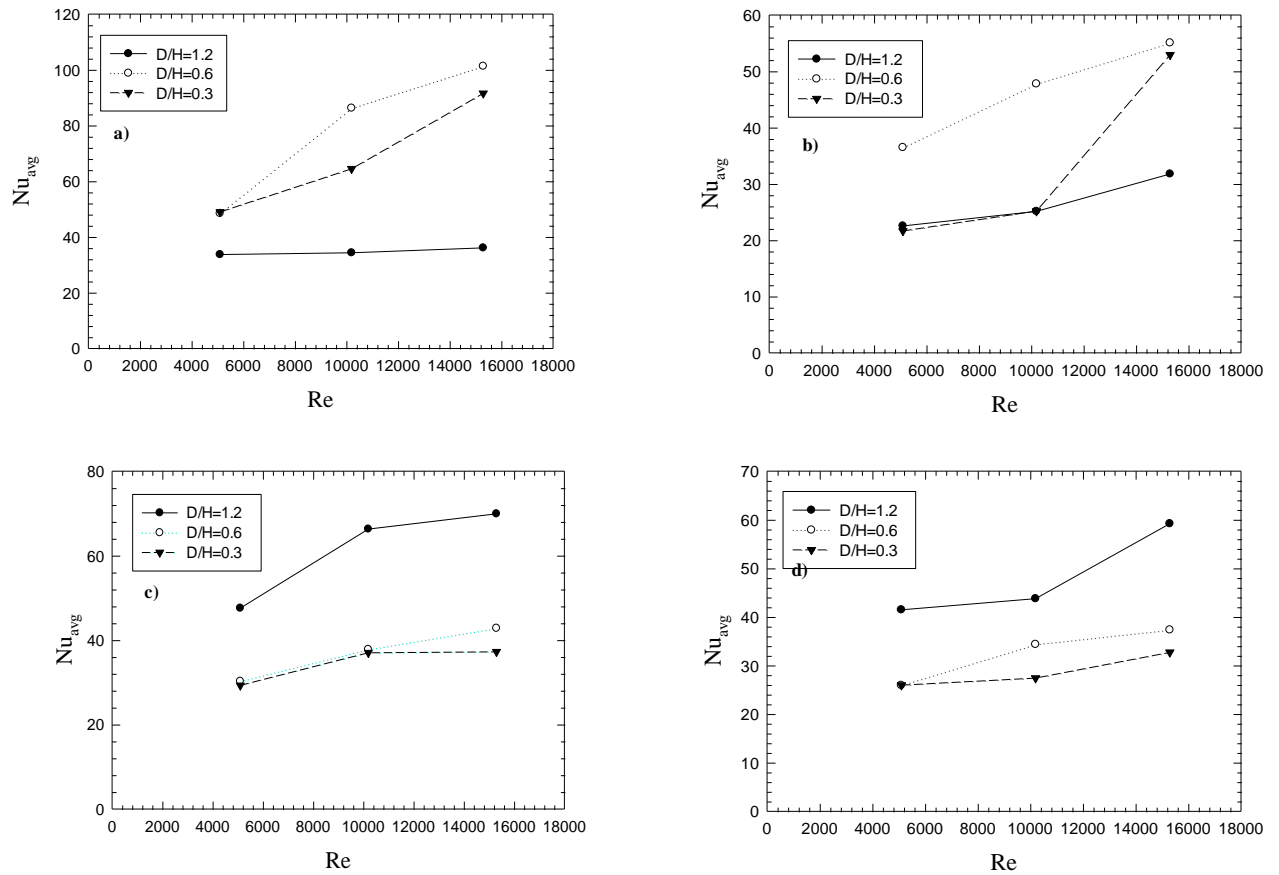


Figure 4. Trend of the ratio Nu_{avg} as a function of Reynolds number for three different configurations: a) $\dot{q} = 510 \text{ W/m}^2$; b) $\dot{q} = 765 \text{ W/m}^2$; c) $\dot{q} = 1020 \text{ W/m}^2$; d) $\dot{q} = 1400 \text{ W/m}^2$.

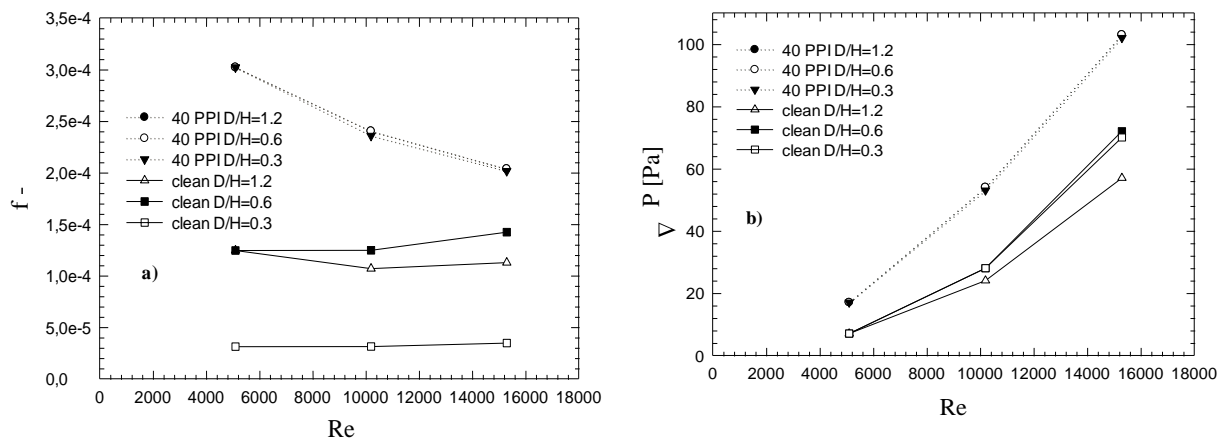


Figure 5. a) Friction factor as a function of Reynolds number; b) pressure drop as a function of Reynolds number.

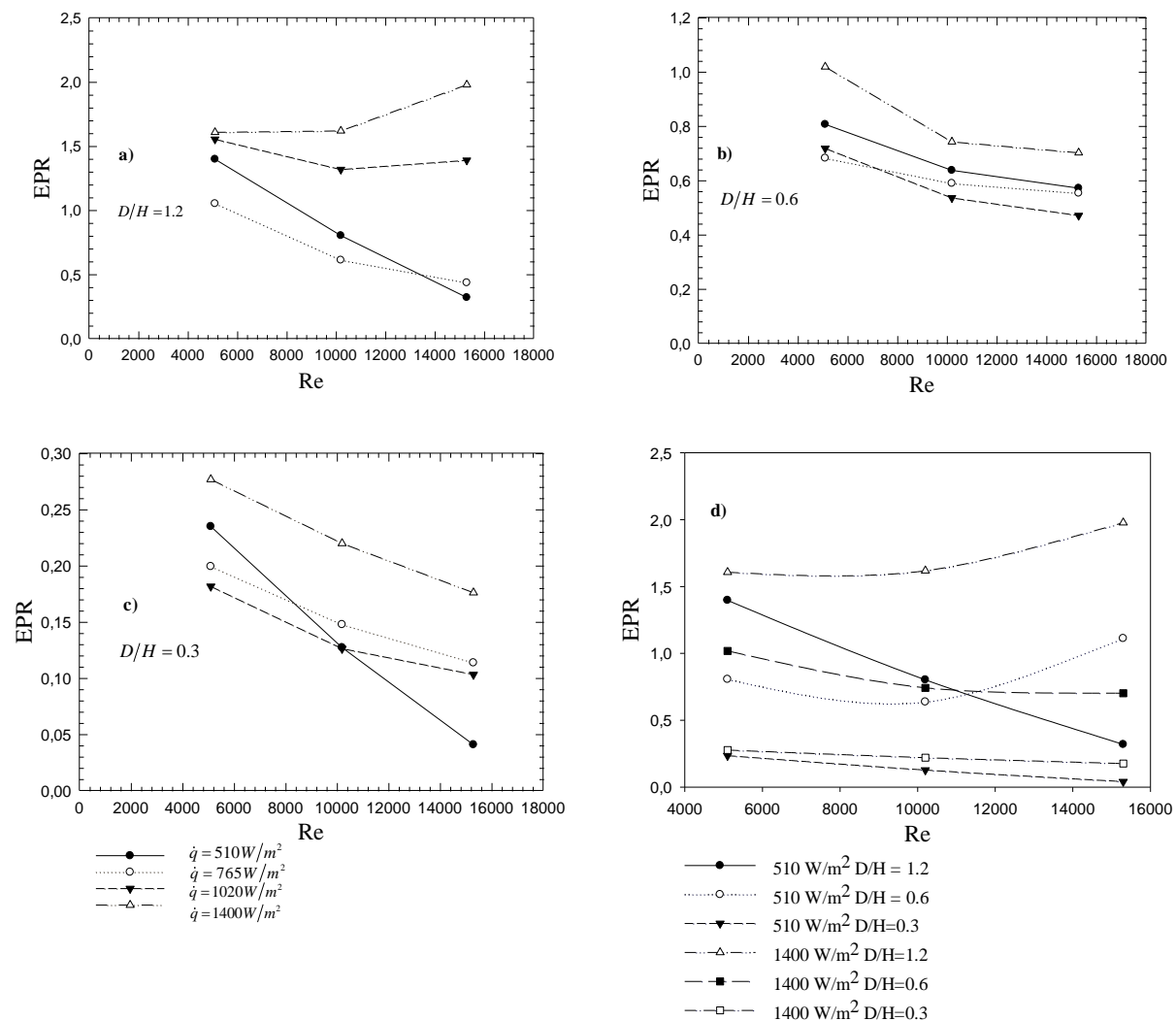


Figure 6. EPR as a function of Reynolds number: a) $D/H = 1.2$; b) $D/H = 0.6$; c) $D/H = 0.3$; d) comparison between two different heat flux.

Figure 6 shows the trend of EPR as a function of Reynolds number and the ratio D/H . It has been demonstrated that the higher efficiency is for higher values of heat flux for all configurations. Besides, the ratio $D/H = 1.2$ has higher values of EPR at lower values of Reynolds number, instead, for higher values of Reynolds number, the EPR decreases for all configurations except for high D/H equal to 1.2 and wall heat flux equal to 1400 W m^{-2} .

5. Conclusions

Main conclusion of this experimental investigations are:

- The use of metal foam improved the heat transfer impinging jet on the heated wall. Reynolds number increase determined a Nusselt number increase and it was detected that for high D/H , equal to 1.2, and low wall heat flux values, the average Nusselt numbers are the highest with respect to the other D/H values.
- It was demonstrated that the metal foam increases the values of friction factor and decreases the ΔP values for all configurations.
- The values of EPR have been demonstrated that metal foam 20 mm thick have an efficiency higher of metal foam 10 and 40 mm thick at lower Reynolds number. At lower values of Reynolds number, the metal foam 10 mm thick have an efficiency higher of those with larger thickness.

References

- [1] Zhao C Y 2012 *International Journal of Heat and Mass Transfer* **55** 3618-32

- [2] Boomsma K, Poulidakos D and Zwick F 2003 *Mech. Mater.* **35** 1161-76
- [3] Han X H, Wang Q, Park Y G, T'Joel C, Sommers A and Jacobi A 2012 *Heat Trans. Eng.* **33** 991-1009
- [4] Leong K C and Jin L W 2006 *Int. J. Heat Fluid Flow* **27** 144-53
- [5] Leong K C and Jin L W 2006 *Int. J. Heat Mass Transfer* **49** 671-81
- [6] Dukhan N, Ramos P D Q, Ruiz E C, Reyes M V and Scott E P 2005 *Int. J. Heat Mass Transfer* **48** 112-20
- [7] Feng S S, Kuang J J, Wen T, Lu T J and Ichimiya 2014 *Int. J. of Heat and Mass Transfer* **77** 1063-74
- [8] Jeng T M and Tzeng S C 2005 *Int. J. of Heat and Mass Transfer* **48** 4685-94
- [9] Jeng T M and Tzeng S C 2007 *Int. J. Therm. Sci.* **46** 1242-50
- [10] Jeng T M and Tzeng S C 2007 *Heat Transfer Eng.* **28** 484-95
- [11] Kim S Y, Lee M H and Lee K S 2005 *IEEE Trans. Compon. Packag. Technol.* **28** 142-48
- [12] Kuang J J et al 2012 *Heat Trans. Eng.* **33** 642-50
- [13] Marafie A et al. 2008 *Numer. Heat Transfer Part A-Appl.* **54** 665-85
- [14] Shih W H, Chou F C and Hsieh W H 2014 *J. of Heat Transfer* **129** 1554-63
- [15] Di Bella E, Azeredo L, Yakkatelli R and Fleischer A 2010 *ASME 2009 Int. Mech. Eng. Congress and Exposition*
- [16] Rallabandi A P, Rhee D H, Gao Z and Han J C 2010 *Int. J. of Heat and Mass Transfer* **53** 4663-71
- [17] Imraan M and Sharma R N 2009 *Int. J. of Refrigeration* **32** 515-23
- [18] Huang L and El Genk M S 1994 *Int. J. of Heat and Mass Transfer* **37** 1915-23
- [19] Kline S and McClintock F. 1953 *Mech Eng* **75** 3-8